Korean J. Chem. Eng., **27**(4), 1049-1055 (2010)
DOI: 10.1007/s11814-010-0208-5

Numerical modeling of volatile organic compound emissions from multi-layer dry building materials

Baoqing Deng*, Songming Tang*, Jeong Tai Kim, and Chang Nyung Kim**,†**

*School of Environmental and Architecture, University of Shanghai for Science & Technology, Shanghai 200093, P. R. China
**College of Engineering (Industrial Liaison Research Institute), Kyung Hee University, Yongin 446-701, Korea
(*Received 22 October 2010 • accepted 22 December 2010*)

Abstract−This paper presents a mathematical model capable of simulating VOCs emission from a multi-layer material. The analytical solutions of the concentration in the air and the emission rate are obtained by Laplace transform and are validated through experiment. The influences of parameters of multi-layer material on the emission of VOCs are investigated in detail. Results show that the inner layer may act as a sink or a source of the top layer, depending on their initial concentrations and partition coefficients. For the case of the inner layer being a source of the top layer, the top layer becomes a barrier layer, reducing the emission rate of VOCs from the source. A low diffusion coefficient and a large thickness may promote the effect of the barrier on the emission rate, which helps to maintain better air quality in an indoor environment. The present solution is a longitudinal extension of a single layer problem, while the emission from multi-source is a transverse extension of a single layer problem.

Key words: VOC Emission, Multi-layer, Dry Building Material, Exact Solution

INTRODUCTION

Many building materials can emit volatile organic compounds (VOCs) that are a severe health threat to occupants of buildings. Recently, much more attention has been paid to the mathematical simulation of the emission of VOCs from building materials. Many authors have investigated the emission of VOCs from a material with a single set of material properties [1-7]. A transient one-dimensional diffusion equation was used to describe the diffusion of VOCs within the material. The concentration of VOCs in the air was described by the mass conservation equation. These studies either solved the governing equations by the finite difference method or obtained analytical solutions. All these research successfully simulated VOCs emission from a single material.

However, there may exist several materials with different material properties in buildings. They can be arranged in a different manner in buildings. One case is that they are placed at the different positions, i.e., multi-source. For example, there exist carpets, furniture and tables etc., in buildings. Many authors have achieved much progress for the modeling of this kind of case [8-11]. The other case is that they share the same position, i.e., a multi-layer material. For example, a carpet is typically made up of carpet fiber, backing, and carpet pad sharing the same position and the same area. Kumar and Little [12] presented a model for the emission of VOCs from double-layer materials. An analytical solution was obtained to compute the concentration distribution in double-layer materials and the concentration in the air. Several authors investigated the case of VOCs emission from multi-layer material [13-15]. They used the finite difference technique to solve the governing equation, while the solution of the model of Kumar and Little [12] was analytical.

In the present study, a physical model capable of predicting the emission of VOCs from a multi-layer material is presented. A simple method to obtain the analytical solution is developed and validated through the experiment carried out by Low et al. [16] in an environmental test chamber. The influences of parameters on the emission of VOCs are also discussed in detail.

MODEL DEVELOPMENT

A chamber with a multi-layer material is shown in Fig. 1. Here, the multi-layer material with a thickness of δ is divided into n layers: $(x_1=0, x_2)$, (x_2, x_3), (x_3, x_4), …, $(x_n, x_{n+1}=\delta)$. The material within each layer is homogeneous. However, each layer may be of different diffusion coefficients and partition coefficients. It is assumed that all layers are in perfect contact with each other. In general, mass transfer takes place not only between the air and the material but also between two adjacent layers depending on the concentration difference in two phases or two layers. According to Fick's law, the transport of VOCs within each layer can be described by a dimensionless

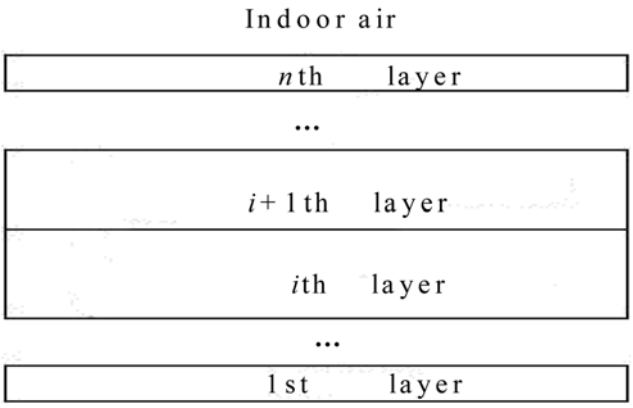

Fig. 1. The structure of a multi-layer material.

†To whom correspondence should be addressed.
E-mail: cnkim@khu.ac.kr

transient one-dimensional diffusion equation as follows:

$$\frac{\partial \psi_i}{\partial \tau} = \Gamma_i \frac{\partial^2 \psi_i}{\partial X^2} \qquad i=1, 2, \ldots, n \tag{1}$$

with

$$\tau = \frac{tD_1}{\delta^2} \quad X = \frac{x}{\delta} \quad \Gamma_i = \frac{D_i}{D_1} \quad \psi_i = \frac{C_i}{C_{10}} \tag{2}$$

where C_i is the concentration in the ith layer, D_i the diffusion coefficient in the ith layer, t the time and x the distance from the bottom of the multi-material. Here i=1 means the base of the material and i=n means the top layer adjacent to the air. Note that the selection of C_{10} and D_1 as the characteristic parameters is arbitrary. A uniform initial condition is given in each layer:

$$\psi_i(t=0) = \psi_{i0} = C_{i0}/C_{10} \tag{3}$$

The diffusion flux at the interface between two adjacent layers keeps continuous, yielding

$$q|_{X_{i+1}} = -\Gamma_i \left.\frac{\partial \psi_i}{\partial X}\right|_{X_{i+1}} = -\Gamma_{i+1} \left.\frac{\partial \psi_{i+1}}{\partial X}\right|_{X_{i+1}} \qquad 1 \le i < n \tag{4}$$

where q is the dimensionless diffusion flux. On the other hand, the concentration is discontinuous at interfaces between two adjacent layers because of phase change, which can be described by Henry's Law:

$$\left.\frac{\psi_i}{K_i}\right|_{X_{i+1}} = \left.\frac{\psi_{i+1}}{K_{i+1}}\right|_{X_{i+1}} \qquad 1 \le i < n \tag{5}$$

where K_i is the material-air partition coefficient for ith layer.

Laplace transform can be used to solve Eqs. (1)-(5). According to Carslaw and Jaeger [17] and taking into account the initial concentration field in each layer and Eq. (5), there exists the following expression in the ith layer:

$$(\lambda \overline{\psi_{i+1}}|_{X_{i+1}}/K_{i+1}, \lambda \overline{q}|_{X_{i+1}})^T = H_i (\lambda \overline{\psi_i}|_{X_i}/K_i, \lambda \overline{q}|_{X_i})^T + G_i \qquad 1 \le i < n \tag{6}$$

with

$$G_i = [\psi_{i0}(1-A_i)/K_i, -E_i \psi_{i0}/K_i]^T \tag{7}$$

$$H_i = \begin{pmatrix} A_i & B_i \\ E_i & A_i \end{pmatrix} \tag{8}$$

$$A_i = \cosh p_i \gamma_i \quad B_i = -\frac{\sinh p_i \gamma_i}{\Gamma_i K_i p_i} \quad E_i = -\Gamma_i K_i p_i \sinh p_i \gamma_i \tag{9}$$

$$p_i = (\lambda/\Gamma_i)^{0.5} \tag{10}$$

where $\gamma_i = X_{i+1} - X_i$ is the dimensionless thickness of *ith* layer, λ the variable of Laplace transform, $\overline{\psi_i}$ and $\overline{q}$ Laplace transforms of the dimensionless concentration in the ith layer and the dimensionless diffusion flux, respectively. By applying Eq. (6) to all layers and performing matrix operation, we can get the following matrix for the *nth* layer adjacent to the air:

$$(\lambda \overline{\psi_n}|_{X_{n+1}}/K_n, \lambda \overline{q}|_{X_{n+1}})^T = \begin{pmatrix} A & B \\ E & A \end{pmatrix} (\lambda \overline{\psi_1}|_{X_1}/K_1, \lambda \overline{q}|_{X_1})^T + \begin{pmatrix} G_c \\ G_q \end{pmatrix} \tag{11}$$

with

$$\begin{pmatrix} A & B \\ E & A \end{pmatrix} = H_n H_{n-1} \cdots H_2 H_1 \tag{12}$$

$$\begin{pmatrix} G_c \\ G_q \end{pmatrix} = G_n + H_n G_{n-1} + H_n H_{n-1} G_{n-2} + \cdots + H_n H_{n-1} \cdots H_2 G_1 \tag{13}$$

Usually the diffusion flux through the base of the material slab is zero:

$$q|_{X_1} = 0 \tag{14}$$

Its Laplace transform is

$$\overline{q}|_{X_1} = 0 \tag{15}$$

Combination of Eqs. (11) and (15) yields

$$\frac{\lambda E}{K_n} \overline{\psi_n}|_{X_{n+1}} = \lambda A \overline{q}|_{X_{n+1}} + E G_c - A G_q \tag{16}$$

The boundary condition at the interface between the air and the top layer is determined by a continuous diffusion flux at the interface and a mass balance in the chamber, which read in the dimensionless form:

$$q|_{X_{n+1}} = Bi_m \left(\frac{1}{K_n} \psi_n|_{X_{n+1}} - \frac{C_a}{C_{10}} \right) \tag{17}$$

$$\frac{1}{C_{10}} \frac{\partial C_a}{\partial \tau} = \beta q|_{X_{n+1}} - \alpha \frac{C_a}{C_{10}} \tag{18}$$

where $Bi_m = h\delta/D_1$, $\beta = L\delta$, $\alpha = N\delta^2/D_1$, C_a is the concentration in the air, L the loading ratio, and N the air exchange rate. Their Laplace transforms are

$$\overline{q}|_{X_{n+1}} = \frac{1}{K_n} Bi_m \overline{\psi_n}|_{X_{n+1}} - Bi_m \frac{\overline{C_a}}{C_{10}} \tag{19}$$

$$\lambda \frac{\overline{C_a}}{C_{10}} = \beta q|_{X_{n+1}} - \alpha \frac{\overline{C_a}}{C_{10}} \tag{20}$$

From Eqs. (16) and (19)-(20), we can get

$$\overline{C_a} = C_{10} \frac{\beta (E G_c - A G_q)}{\lambda [(Bi_m^{-1}(\lambda+\alpha)+\beta)E - (\lambda+\alpha)A]} \tag{21}$$

$$\overline{q}|_{X_{n+1}} = \frac{(\lambda+\alpha)(E G_c - A G_q)}{\lambda [(Bi_m^{-1}(\lambda+\alpha)+\beta)E - (\lambda+\alpha)A]} \tag{22}$$

The solutions of Eqs. (21) and (22) can be derived by the use of the inversion theorem. The solution process can be referred to Deng and Kim [7]. For simplicity, only the ultimate solution is given here.

$$C_a = C_{10} \beta \sum_{k=1}^{\infty} Y_k e^{-r_k^2 \tau} \tag{23}$$

$$q|_{X_{n+1}} = \sum_{k=1}^{\infty} (\alpha - r_k^2) Y_k e^{-r_k^2 \tau} \tag{24}$$

with

$$Y_k = \frac{1}{r_k^2 A + (\alpha - r_k^2) A' - Bi_m^{-1} E - [Bi_m^{-1}(\alpha - r_k^2) + \beta] E'} \frac{(E G_c - A G_q)_{\lambda = -r_k^2}}{} \tag{25}$$

where A′ and E′ are computed according to the following equation:

$$\begin{pmatrix} A' & B' \\ E' & F' \end{pmatrix} = \frac{d}{d\lambda}(H_n H_{n-1} \cdots H_2 H_1) \tag{26}$$

The dimensionless r_k are the positive roots of

$$[Bi_m^{-1}(\alpha - r_k^2) + \beta]E|_{\lambda=-\eta_k^2} - (\alpha - r_k^2)A|_{\lambda=-r_k^2} = 0 \tag{27}$$

From Eqs. (23)-(27), the concentration in the air and the emission rate at the material-air interface can be computed. In general, terms A and E are very complicated for cases of n>2. Thus, complete expressions of Eqs. (23)-(27) would be very tedious, but they are easy to perform by computer code. Since the present model is developed for a multi-layer material, it also applies to the cases of a single-layer and a double-layer. When n=1 is taken, Eqs. (23) and (27) reduce to those of Deng and Kim [7].

In the solution of the emission from a multi-layer material, some matrices are used, i.e., Eqs. (8), (12) and (26). Eq. (8) is the characteristic matrix of the single layer of a multi-layer material. Eqs. (12) and (26) are the characteristic matrices of the whole multi-layer material. All these characteristic matrices are 2×2 matrices, meaning that the characteristic matrix does not change with the number of layers of the multi-layer material. However, the situation is not so for the case of multi-source emission. For each source, the characteristic matrix is also a 2×2 matrix, i.e., Eq. (16) of Deng et al. [8]. When n sources exist, the characteristic matrix becomes an (n+1)×(n+1) matrix, i.e., Eq. (23) of Deng et al. [8]. So, the emission from a multi-layer material is a longitudinal extension of a single layer problem while the emission from multi-source is a transverse extension of a single layer problem. Obviously, these features accord with the arrangement of the materials in two cases.

All diffusion coefficients, layer thickness, partition coefficients and initial concentrations in the material can be obtained from experiments. As for the gas-phase mass transfer coefficient, some empirical relations can be adopted. For laminar flow, there exists [18]

$$Sh = 0.664 Sc^{1/3} Re^{1/2} \tag{28}$$

where $Sh = hl/D_a$ is Sherwood number, $Sc = v/D_a$ Schmidt number, $Re = ul/v$ Reynolds number, v the kinematic viscosity of the air, u the velocity of the air over the material, l the characteristic length of the material, and D_a the diffusion coefficient of VOCs in the air.

VALIDATION OF THE MODEL

The experimental data of the emission of VOCs from a carpet - adhesive assembly [16] is used to validate the prediction of the present model. The experiments were carried out in a small-scale stainless steel chamber of 0.4 m^3 following the rules of ASTM D 5116-97. In the experiments, the adhesive was applied on the concrete slab and the carpet was placed on the adhesive. The loading ratio was 0.31 m^{-1} and the air exchange rate was 1.0 h^{-1}. The emission rates of decane from carpet - adhesive assembly at air velocities of 0.04 m-s^{-1} (test 4) and 0.1 m-s^{-1} (test 5) were used to examine the model performance. The model parameters taken from Haghighat and Huang [13] are listed in Table 1. The computed emission rates of decane at air velocities of 0.04 m-s^{-1} and 0.1 m-s^{-1} are depicted in Figs. 2-3. During the early stage (<20 h), some discrepancies exist between the experimental data and the computed data for both cases. It may be ascribed to the instability and partial mixing in the chamber in the early stage. However, in the long term, a good agreement is obtained between the experimental data and the computed data.

On the other hand, a comparison between the single-layer model [7] and the present multi-layer model is carried out. The selected experiment was performed by Yang et al. [19]. The corresponding parameters for the single-layer model are: $D = 7.65\times10^{-11}$ m^2s^{-1}, K= 3,289, $C_0 = 5.28\times10^7$ μg-m^{-3} and δ=0.0159 m. As for the multi-layer

Table 1. Model parameters for the validation

Material		Thickness (mm)	C_{i0} (mg-m^{-3})	K_i	D_i (m^2s^{-1})
Carpet		2.0	0	1.46e+4	8.0e-11
Adhesive	Test 4	4.37e-1	3.6e+6	1.46e+4	2.92e-10
	Test 5	4.08e-1			8.92e-12

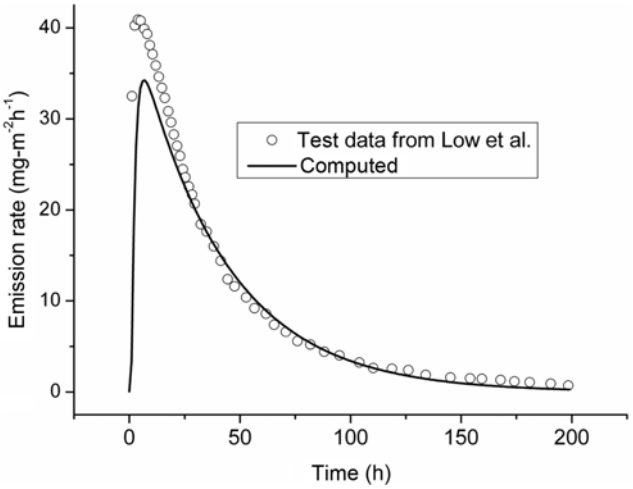

Fig. 2. Comparison of the emission rate of decane at velocity of 0.04 m-s^{-1}.

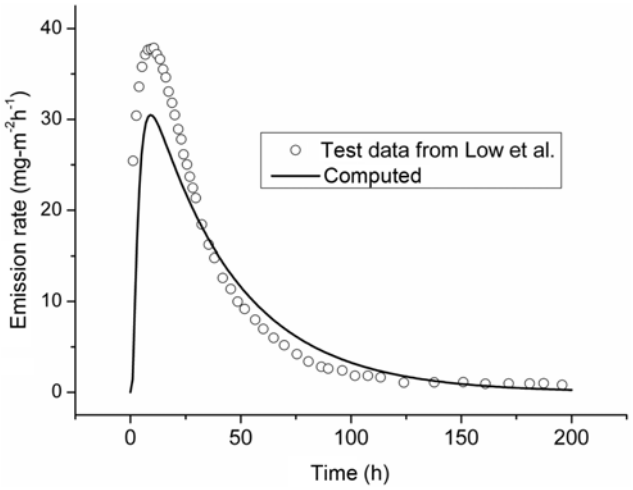

Fig. 3. Comparison of the emission rate of decane at velocity of 0.1 m-s^{-1}.

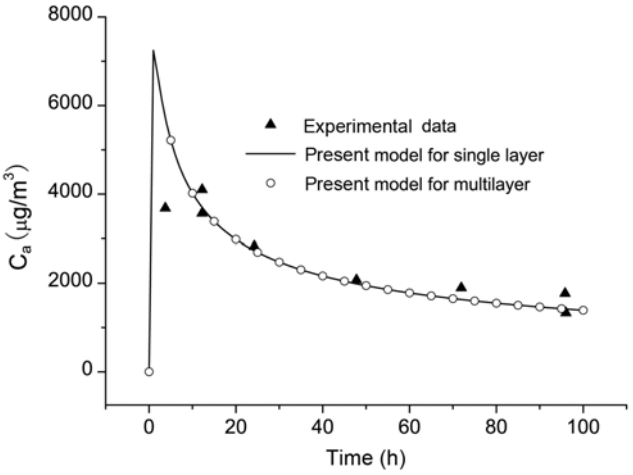

Fig. 4. Comparison of the single-layer model and the multi-layer model.

model, the material is divided into three layers with the thickness of 0.012 m, 0.002 m and 0.0019 m, respectively. Other parameters are the same as those for the single-layer model. The computed VOCs concentrations in the air with two methods are depicted in Fig. 4. The computed VOCs concentrations with two methods totally coincide with each other showing that the proposed multi-layer model is reasonable.

PARAMETRIC ANALYSIS

The multi-layer model is applied to investigate the influence of parameters of the multi-material on the VOCs concentration in the air and the emission rate at the material-air interface. A three-layer material is considered here.

1. The Influence of Partition Coefficient

In Fig. 5 and Fig. 6 are shown the influences of the partition coefficient on VOCs emission. The parameters are listed in Table 2. All five cases depict the same concentrations and the same emission rates in the first hour, which shows that the emission during this stage is dominated by the top layer. From t=1 h to t=100 h, the concentration in the air and the emission rate for the cases of $K_1=10K_2=K_3$ and $10K_1=K_3=K_3$ are greater than those for the case of $K_1=K_2=K_3$. This is because the equivalent air-phase concentration difference between the middle layer and the top layer for these two cases is positive and much greater than that for the case $K_1=K_2=K_3$. It is just reverse for the cases of $K_1=0.1K_2=K_3$ and $0.1K_1=K_2=K_3$. The equivalent air–phase concentration difference between the middle layer and the top layer is negative for these two cases and its absolute value is much greater than that for the case $K_1=K_2=K_3$. The bottom layer plays the same role as the middle layer in the emission. The difference is that its effect is weaker than that of the middle layer. The inner layer can be a source or a sink of the top layer depending on their initial concentrations and partition coefficients. It is much different from a single-layer material in which the interior of the material is always a source of the surface. If the inner layer is a sink for the top layer, it would help to reduce the concentration of VOCs in the air and prolong the existence of VOCs in indoor environment compared to the case of only the top layer. If the inner layer is a source for the top layer, the top layer would be a barrier and may reduce the emission of VOCs from the inner layer compared to the case of only the inner layer.

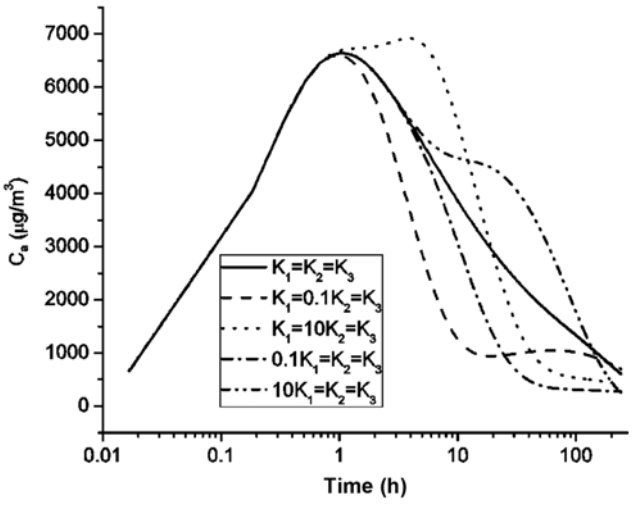

Fig. 5. The influence of partition coefficient on VOCs concentration in the air.

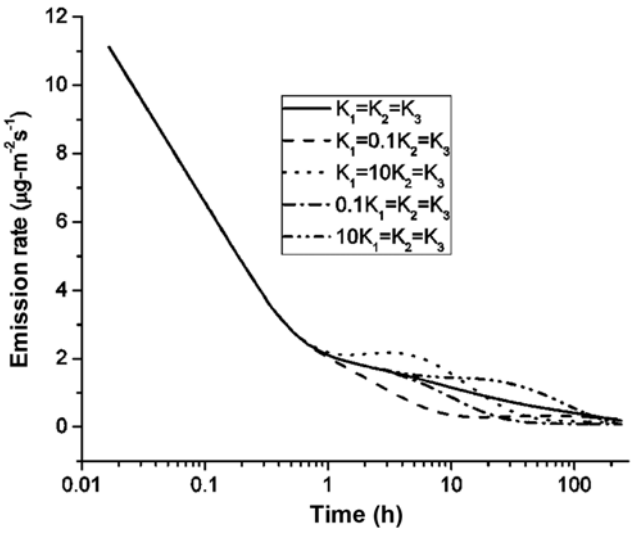

Fig. 6. The influence of partition coefficient on the emission rate.

Table 2. Parameters for the effect of partition coefficient

	D (m^2s^{-1})	K	Thickness (mm)	C_0 (mg-m^{-3})
Top layer		3289	2	
Middle layer	7.65×10^{-11}		2	5.28×10^{7}
Bottom layer			6	

2. The Influence of Material Thickness

When VOCs exist in the inner layer, the top layer becomes a barrier of the emission of VOCs. Fig. 7 illustrates the effect of the top layer on the emission of VOC from the middle layer. The parameters are listed in Table 3. Even if there is only a minor variation in the thickness of top layer, VOCs concentration in the air varies sig-

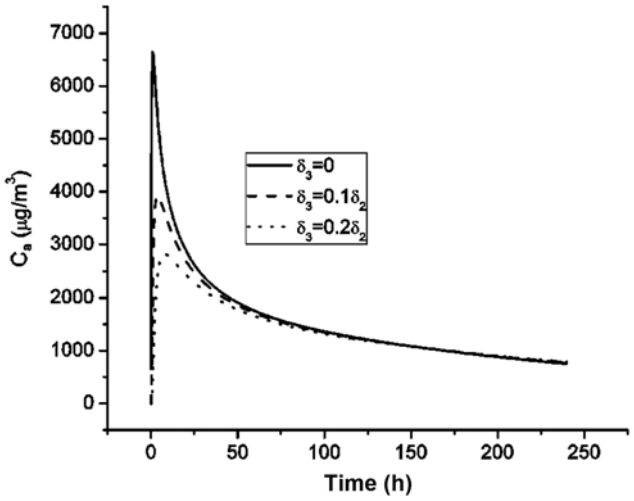

Fig. 7. The influence of the thickness of the top layer on VOCs concentration in the air.

Table 3. Parameters for the effect of layer thickness

	D (m^2s^{-1})	K	Thickness (mm)	C_0 (mg-m^{-3})
Top layer				0
Middle layer	7.65×10^{-11}	3289	6	5.28×10^{7}
Bottom layer			6	0

nificantly. Because of the zero concentration of the top layer, the VOCs concentration in the air keeps a small value close to zero for a long time when the thickness of top layer is not zero. Thus, the VOCs concentration in the air could be reduced significantly by adding a thin covering layer on the surface of VOCs source. Although this method would prolong the existence of VOCs in an indoor environment, it offers a better air quality for a long time because of a low concentration in the air.

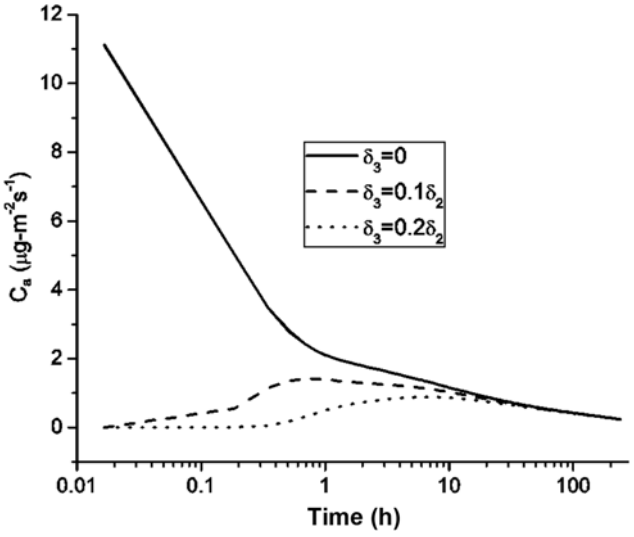

Fig. 8. The influence of the thickness of the top layer on the emission rate.

Table 4. The first five values of r_k for different thicknesses

	δ_3=0.0δ_2	δ_3=0.1δ_2	δ_3=0.2δ_2
1	1.519583	1.521945	1.524099
2	4.559164	4.566183	4.572591
3	7.599995	7.611691	7.62221
4	10.64334	10.65905	10.67345
5	13.68934	13.70897	13.72696

In Fig. 8 is shown the effect of the thickness of the top layer on the emission rate. The top layer significantly reduces the emission rate. Before t=1 h, the curve for δ_3=0 decreases steeply while the curves for other two cases keep a zero value. After t=1 h, the emission rate for δ_3=0 continues to decline with a small slope, while the emission rates for other two cases begin to increase slowly. After a long time, all of the three emission rates keep a very low level almost without harm to indoor air quality.

Table 4 gives the first five values of r_k. With the increase of the thickness of top layer, the values of r_k increase. Since r_k are located at the position of the exponent in Eqs. (23)-(24), the VOCs concentration and the emission rate would decrease with the increase of the thickness of top layer. Although the values of r_k do not change much, the VOCs concentration and the emission rate change much, which is due to the enlargement of the exponential function.

3. The Influence of Diffusion Coefficient

Since a thin layer can reduce the emission rate of VOCs from a source, a multi-material with $10\delta_3=\delta_1=\delta_2$ is chosen to investigate the influence of diffusion coefficient on the VOCs emission. The same initial concentrations and the partition coefficients are taken for three layers.

Fig. 9 illustrates the influence of diffusion coefficients in the middle layer on VOC emission. The parameters are listed in Table 5. Before t=3 h, the concentration in the air for all cases is the same showing the emission is governed totally by the top layer. After t= 3 h, the concentration of VOCs in the air increases with the increase of the diffusion coefficient in the middle layer. It means that the middle layer acts as an additional source to the top layer. The emission rates

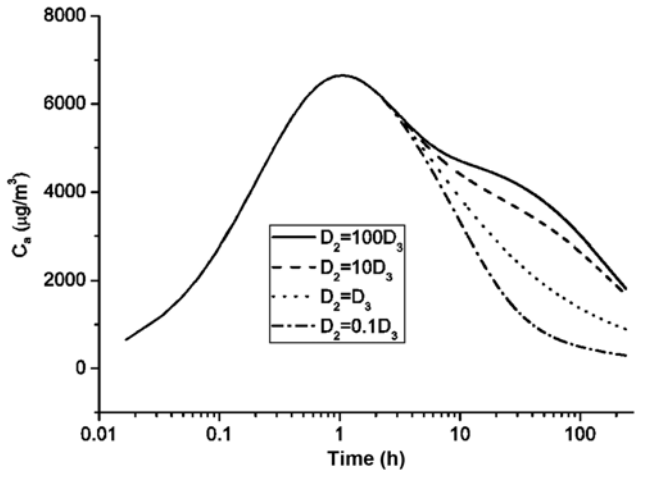

Fig. 9. The influence of diffusion coefficient of the middle layer on VOCs concentration in the air.

Table 5. Parameters for the effect of diffusion coefficient

	D (m^2s^{-1})	K	Thickness (mm)	C_0 ($mg\text{-}m^{-3}$)
Top layer	7.65×10^{-11}		0.6	5.28×10^7
Middle layer		3289	6	5.28×10^7
Bottom layer	7.65×10^{-11}		6	5.28×10^7

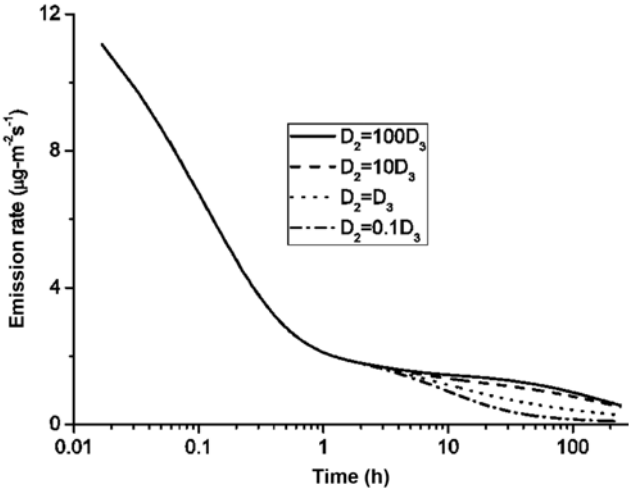

Fig. 10. The influence of diffusion coefficient of the middle layer on the emission rate.

are depicted in Fig. 10. It also demonstrates that a higher diffusion coefficient can lead to a higher emission rate at the material-air interface. This is because a high diffusion coefficient means a low resistance to the diffusion of VOCs through the top layer.

CONCLUSION

This paper presents a mathematical model capable of predicting the emission of VOCs from multi-layer materials. Both the diffusion within the material and the mass transfer resistance through the air boundary layer are taken into account. A simple solution method is developed based on the equivalent air-phase concentration and Laplace transform. The concentration in the air and the emission rate at the material-air interface can be expressed by two infinite series with good convergence.

The present solution is validated through the experiment of Low et al. [16] in an environmental test chamber. A comparison between the single-layer model and the present multi-layer model is performed with respect to the emission of VOCs from a single-layer material in an environmental test chamber [19]. Totally the same results are obtained from the single-layer model and the multi-layer model. The influence of parameters on VOCs emission is investigated in detail. The inner layer may act as a source or a sink of the top layer, depending on their initial concentrations and partition coefficients. When a barrier layer is placed on the surface of an emission source, the existence of a very thin covering layer can reduce the emission of VOCs from the source. Moreover, a low diffusion coefficient in the barrier layer can promote this reduction. Thus, it implies a simple way to reduce the concentration of VOC in the air to get an acceptable air quality.

ACKNOWLEDGEMENTS

This research work was partly sponsored by the Leading Academic Discipline Project of Shanghai Municipal Education Commission (No. J50502), and partly supported by the Basic Science Research Program through the National Research Foundation of Korea (NRF) funded by the Ministry of Education, Science and Technology (No. 2009-0063383).

NOMENCLATURE

Bi_m : $Bi_m=h\delta/D_1$
C_i : the concentration in the ith layer
C_a : the concentration in the air
D_a : the diffusion coefficient of VOCs in the air
D_i : the diffusion coefficient in the ith layer
h : gas phase mass transfer coefficient
K_i : the material-air partition coefficient for *ith* layer
L : the loading ratio, i.e., the ratio of surface area of material to the volume of chamber
N : the air exchange rate
l : the characteristic length of material
r_k : positive roots
q : dimensionless diffusion flux
t : time
u : the velocity of the air over the material
v : the kinematic viscosity of air
x : the distance from the bottom of multi-material
X : dimensionless distance from the bottom of multi-material
α : $\alpha=N\delta^2/D_1$
β : $\beta=L\delta$
γ_i : the dimensionless thickness of *ith* layer
Γ_i : dimensionless diffusion coefficient
δ : the thickness of the multi-layer material
τ : dimensionless time
Ψ_i : the dimensionless concentration in the *ith* layer
λ : the variable of Laplace transform
Sh : Sherwood number
Sc : Schmidt number
Re : Reynolds number

REFERENCES

1. J. C. Little, A. T. Hodgson and A. J. Gadgil, *Atmospher. Environ.*, **28**, 227 (1994).
2. S. S. Cox, J. C. Little and A. T. Hodgson, *Environ. Sci. Technol.*, **36**, 709 (2002).
3. D. M. Shin, C. N. Kim and D. S. Kim, *J. SAREK*, **15**, 40 (2003).
4. H. Huang and F. Haghighat, *Build. Environ.*, **37**, 1349 (2002).
5. Y. Xu and Y. P. Zhang, *Atmospher.Environ.*, **37**, 2497 (2003).
6. Y. Xu and Y. P. Zhang, *Atmospher. Environ.*, **38**, 113 (2004).
7. B. Q. Deng and C. N. Kim, *Atmospher. Environ.*, **38**, 1173 (2004).
8. B. Q. Deng, B. Yu and C. Kim, *Chinese Sci. Bull.*, **53**, 1100 (2008).
9. F. Li and J. L. Niu, Proceedings of Healthy Buildings (2006).
10. F. Li and J. L. Niu, *Atmospher. Environ.*, **41**, 2344 (2007).

11. H. P. Hu, Y. P. Zhang, X. K. Wang and J. C. Little, *Int. J. Heat Mass Transfer*, **50**, 2069 (2007).
12. D. Kumar and J. C. Little, *Atmospher. Environ.*, **37**, 5529 (2003).
13. F. Haghighat and H. Huang, *Build. Environ.*, **38**, 1007 (2003).
14. L. Z. Zhang and J. L. Niu, *Build. Environ.*, **39**, 523 (2004).
15. Y. Zhang, H. Hu and X. Wang, Proceeding of the 4th International Conference of Heating, Ventilating and Air-conditioning (2003).
16. J. M. Low, J. S. Zhang, E. G. Plett and C. Y. Shaw, *ASHRAE Transactions*, **104**, 1281 (1998).
17. H. S. Carslaw and J. C. Jaeger, *Conduction of heat in solids*, Oxford University Press (1959).
18. F. M. White, *Heat Mass Transfer*, Addison-Wesley (1988).
19. X. Yang, Q. Chen, J. S. Zhang, R. Magee, J. Zeng and C. Y. Shaw, *Build. Environ.*, **36**, 1099 (2001).